Available online at www.sciencedirect.com
SCIENCE DIRECT®
International Journal of Heat and Mass Transfer 48 (2005) 2516–2528
International Journal of HEAT and MASS TRANSFER
www.elsevier.com/locate/ijhmt

Visualization and mechanisms of pool boiling of propane, isobutane and their mixtures on enhanced tubes with reentrant channels

Yuming Chen *, Manfred Groll, Rainer Mertz, Rudi Kulenovic

Institute of Nuclear Technology and Energy Systems (IKE), University of Stuttgart, Pfaffenwaldring 31, 70569 Stuttgart, Germany

Received 3 May 2004; received in revised form 8 September 2004
Available online 29 March 2005

Abstract

Visualization experiments were carried out for boiling of propane, isobutane and their mixtures on a smooth and four reentrant enhanced tubes. The results shown by the video pictures indicate a strong mixture effect on nucleation and evaporation processes on the enhanced surfaces. The fluid physical properties also influence the bubble behavior and consequently affect the heat transfer performance. The effects of reentrant enhanced surface geometries are complicated and closely related to mixture effects, fluid properties and working conditions. Based on the analysis of the available visualization results, the different heat transfer performance for different enhanced surfaces and especially the difference between pure fluids and mixtures, as shown in an accompanying paper [Chen et al., Int. J. Heat Mass Transfer, in press], are partially explained.

Keywords: Pool boiling; Mixtures; Propane/isobutane; Enhanced tube; Visualization; Boiling mechanisms

1. Introduction

As shown in [1], the boiling heat transfer performance of a reentrant enhanced surface is quite different from that of a smooth surfaces. This is due to the different boiling mechanisms. The most important difference lies in the way by which the vapor is generated. For smooth surfaces, the vapor is generated through the nucleation and growth of individual bubbles. For enhanced tubes, the vapor is mainly generated by the evaporation inside the channels and exists in the form of vapor columns [2–4] from which vapor bubbles are generated.

Based on the visualization experiments for horizontal single channels under a perforated flat surface, Nakayama et al. [2] proposed three modes of channel behavior, viz., the *dried-up mode*, the *suction-evaporation mode* and the *flooded mode*. In the dried-up mode, the channel space is filled with vapor and vaporization occurs on the outer surface, which is likely to happen at high fluxes on a surface with small pores. In the flooded mode, most of the channel space is occupied by liquid, which is likely to happen in case of big pore diameters (0.5 mm) [5], or in sub-cooled boiling [3]. It was found that once a channel is activated, it is in the suction-evaporation mode in which liquid is sucked into the channel space through

* Corresponding author. Fax: +49 711 6852010.
E-mail address: chen@ike.uni-stuttgart.de (Y. Chen).

0017-9310/$ - see front matter © 2005 Elsevier Ltd. All rights reserved.
doi:10.1016/j.ijheatmasstransfer.2004.10.039

inactive pores by pumping action of bubbles growing at active pores [2]. Chien and Webb's [3] observations of boiling on tubes having multiple channels confirm that suction-evaporation is the main mode of boiling on this kind of surfaces.

Trewin et al. [6] showed that, for a Turbo-B tube, in the fully established nucleate boiling range, the most influential heat transfer mechanism takes place in the subsurface channels alone, where thin-film evaporation dominates and nucleate boiling is suppressed. This is indicated by the fact that the heat transfer coefficient is a weak function of heat flux (wall superheat). The visualization experiments also indicated that thin-film evaporation (on the channel wall, especially, in the corners) is the principle boiling mechanism for structured reentrant surfaces [2,3,7,8]. However, some others suggested that the promotion of nucleation sites on the channel surface is the main mechanism (e.g. [9]), which was given, without experimental evidence, to explain the high performance of the enhanced surfaces.

Due to the highly efficient thin-film evaporation inside the subsurface channels, generally, no nucleation sites were found on the outer non-pore area [4]. Experimental results also show a much higher ratio of latent heat flux to total heat flux for enhanced tubes than for smooth tubes [4,5], and the sensible heat transfer is also greatly improved for enhanced tubes [4,10]. The latter was attributed to the higher active site (pore) density of enhanced surfaces [11,12] which, however, seems unlikely, since a very high active site density (up to $10^7\ m^{-2}$ [13] and 10^8–$10^9\ m^{-2}$ near CHF [14]) was found for smooth surfaces, which can be several ten times higher than the total pore density for the Thermoexcel-E and Turbo-B surfaces (refer [4]). Thome [10] concluded that the liquid-phase convection inside the enhanced matrix is the dominant factor, i.e. the outflow of the superheated liquid from the channels. This conclusion may be more applicable to the surfaces with big openings such as Gewa-K or Gewa-T and also for the High Flux surface, where the outflow of the liquid from the channels can easily happen, however, this was not observed for surfaces like Thermoexcel-E [3]. In [4], the much higher departure diameter as well as the higher bubble growth rate and bubble rise velocity for an enhanced surface were thought to be the main reason for the augmentation of sensible heat transfer.

The heat transfer performance of an enhanced surface strongly depends on the surface geometries in connection with fluid properties and working conditions [1,11]. For reentrant surfaces, the best heat transfer performance happens at low or moderate heat fluxes. With increasing heat fluxes, the boiling curve passes through a maximum which indicates that there is an optimal channel geometry and pore size for a definite heat flux [2,5,9,15,16]. The heat flux corresponding to the maximal heat transfer coefficient was called dry-out heat flux (DHF). Above DHF, evaporation occurs only on the outer surface [16] which, however, needs to be confirmed by visualization experiments.

Based on experimental results, Trewin et al. [6] concluded that the size of the openings has very little influence on the boiling curve for a Turbo-B tube. However, some others did show the influences of surface geometries on boiling heat transfer for structured reentrant surfaces [2,15–17]. Nakayama et al. [2] showed that, for a Thermoexcel-E surface having pores of different sizes, the most populous pores govern the rate of heat transfer at moderate and high heat fluxes; at low levels of heat flux, pores of the largest size play an important role in heat transfer. Chien and Webb [16] showed that, at a low heat flux, tubes with smaller "total open area" (defined as the sum of pore areas) yield higher heat transfer coefficients, while for a high heat flux, tubes with larger total open area perform better. At a certain reduced heat flux, part of the channels will become flooded and the performance will be reduced. Smaller pore size inhibits flooding at reduced heat fluxes, while the DHF is lower. It was also shown that, the heat transfer coefficient increases with increasing fin height, which is significant for small fin heights. The effect of fin pitch is not as significant as the combination of pore diameter and pore pitch. Small fin base radius results in higher heat transfer performance [15]. Ma et al. [17] also found that the pore size is the most important geometry parameter and that the optimum pore size is different for different fluids.

The above findings are all based on experiments with pure fluids. As mentioned in [1], only a few studies have been carried out for boiling of mixtures on the reentrant enhanced surfaces. There is a lack of understanding of the mechanisms and little is known concerning the visual phenomena for enhanced boiling of mixtures. Even without mixture effects, the combined effects of surface geometries and fluid properties are not well understood. The main aim of this study is to provide and analyze the video pictures obtained by visualization experiments to show the effects of mixtures, surface geometries, fluid properties and working conditions on bubble and channel behavior for reentrant surfaces. Thereby, the significantly different heat transfer performance, as shown in the accompanying paper [1], for different enhanced surfaces and different fluids, especially the differences between pure fluids and mixtures, will be partially explained.

2. Test surfaces and working fluids

Five kinds of carbon steel (ST35.8) tubes with outer diameter (ϕ) of about 19 mm and length of about 115 mm are used, one conventional smooth tube (R_a = 1.1 μm) and four structured reentrant tubes with

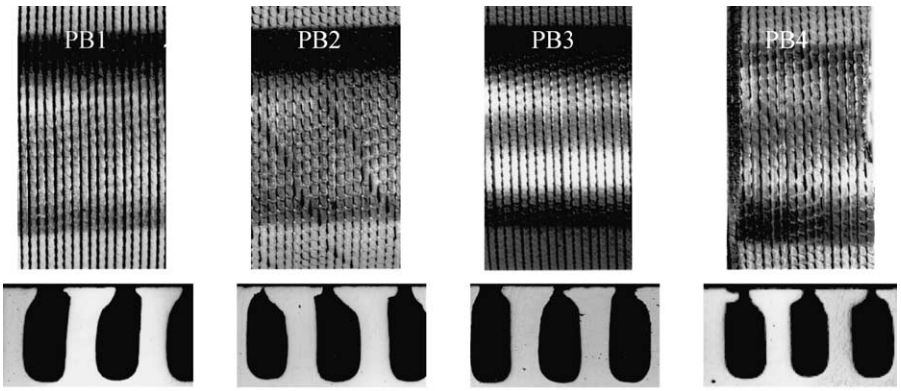

	ϕ	a	b	c	d	e	f	Deviation of "e" (%)
PB1	19.22	0.279	0.694	0.169	0.220	0.164	0.812	12.8
PB2	19.14	0.305	0.686	0.205	0.218	0.081	0.794	32.3
PB3	19.16	0.290	0.679	0.168	0.228	0.076	0.811	47.5
PB4	19.17	0.299	0.711	0.184	0.209	0.062	0.862	38.4

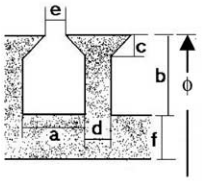

Fig. 1. Enhanced surfaces and geometric data (upper photo: tube surface; lower photo: cut-view of subsurface channel).

sub-surface channels and surface openings named PB1 to PB4 (Fig. 1), respectively. PB1 has the biggest mean opening, while PB4 has the smallest mean opening. Furthermore, PB4 has the biggest fin height (i.e., "*b*") and smallest fin thickness (i.e., "*d*"), therefore it has the biggest channel surface area per unit tube length. Tubes PB1 and PB3 resemble more the Gewa-T tubes, because instead of individual pores, they have practically throughout circumferentially open slits with widths in the range of about 0.05–0.2 mm for PB1 and about 0.03–0.12 mm for PB3; the widths differ from slit to slit and also along the circumference of the individual slits (for comparison: the Gewa-T tubes have relatively uniform slits of about 0.4 mm in width). Tubes PB2 and PB4 are more similar to the Thermoexcel-E tubes. With the exception of a few slits all around the circumference, the sub-surface channels are connected via approximately elliptic pores to the surroundings. The pore areas are in the range of about (0.02–0.09 mm) (0.3–1 mm) for PB4. For PB2 there are many big pores with the size of about 0.2×1 mm spreading regularly on the surface.

Pure propane N35, pure isobutane N35 and three propane and isobutane mixtures are used as working fluids. The mixtures have mass fractions of ***propane*** of ***5%***, ***50%*** and ***95%*** which are called ***5–95% mixture***, ***50–50% mixture*** and ***95–5% mixture***, respectively.

Visualization experiments are carried out by using a high-speed video system (Kodak Ektapro HS motion analyzer 4550, CCD-sensor: 256×256 pixel, full-frame: 4500 frames/s). A uniform backlight with a white cold light source (120 000 lux, 5600 K) is used for illumination. The digital image processing is done by the self-developed software C-library (IKE_DBV). Refer [1] for details of the experimental set-up.

3. Characteristics of bubble formation on enhanced tubes

Due to the buoyancy force, at low heat fluxes ($q < 10$ kW/m^2), most of the active pores focus on the top surface of the enhanced tubes (Fig. 2a). With increasing heat fluxes, more and more active pores are found on the lower part of the surfaces (Fig. 2b). The initial bubbles generated on the side wall are smaller than those on the top surface. The bubbles growing on the bottom surface generally merge to form bigger bubbles and then slide along the side wall, taking away with them the bubbles on their way.

The size of bubbles is mainly influenced by surface tension, system pressure and heat flux, as shown in Fig. 3a–d for the enhanced tube PB4. The isobutane bubbles (Fig. 3b) are generally bigger than propane bubbles (Fig. 3a) due to the higher surface tension of isobutane. Since the pore sizes on the enhanced surfaces are not uniform, but rather follow a certain distribution, the increasing vapor pressure inside the channels resulting from increasing heat flux enables more smaller pores to be activated, from which smaller bubbles are generated (compare Fig. 3b and c). The increase of system pressure reduces the surface tension of the fluid, as a result the departure diameter decreases (compare Fig. 3b and d).

A comparison of bubble departure diameters for the smooth and enhanced tubes is shown in Fig. 4. The data

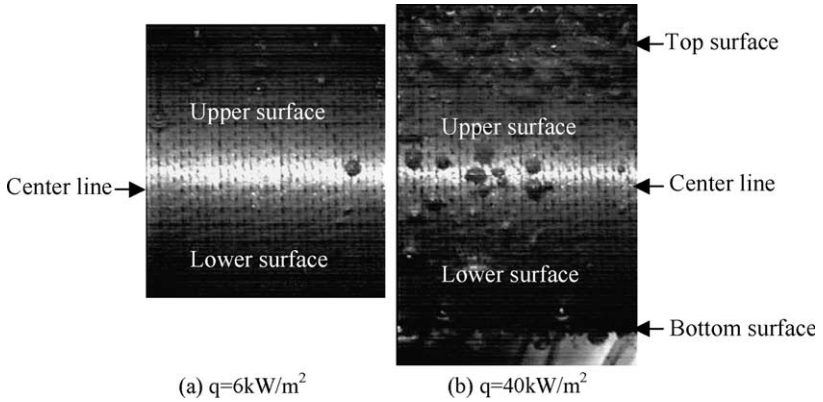

Fig. 2. Bubbles growing on the enhanced surface (PB4, propane, $T_S = 283$ K. Photo shown in (b) is the combination of two photos).

shown for the smooth tube are measured from several individual nucleation sites, and the data shown for enhanced tubes are the mean values of measurements from 10 to 20 sites. The bubble departure diameters for the smooth tube (typically 0.2 mm) are much smaller than those for the enhanced tubes (typically 1.2 mm). For the enhanced tubes, the departure diameters for the mixtures are bigger than those for propane (except for the 95–5% mixture) and smaller than those for isobutane. This is mainly attributed to the effects of surface tension. The data shown for PB1 are similar to those for PB4. In fact, no big difference is found for the bubble sizes for all tubes PB1-4.

4. Boiling initiation

Boiling hysteresis is found not only for the smooth tube, but also for the enhanced tubes, especially during boiling of mixtures (Fig. 3 in [1]). For the smooth tube during boiling of isobutane, natural convection schliere can be seen for $q \leqslant 5$ kW/m^2 (Fig. 5a). At $q = 5$ kW/m^2, bubbles begin to initiate from certain parts of the surface and the active sites spread gradually around the whole surface. The initiated bubbles (around 0.8 mm in diameter) are much bigger than those generated under normal conditions (about 0.2 mm). For descending heat flux, nucleation can be seen even at heat fluxes down to 1 kW/m^2.

For boiling of pure components on the enhanced tubes, natural convection schliere was not recorded (possibly does not exist). Fig. 5b shows the boiling initiation on PB1 for the 50–50% mixture. Natural convection schliere can be seen for $q \leqslant 10$ kW/m^2 (the flow pattern near the top of the photos is influenced by the unheated upper tube). The convection flow which is greatly influenced by the outflow of hot liquid from the subsurface channels through the openings, is much stronger (indicated by the schliere) than that on the smooth surface. Boiling is initiated at $q \approx 10$ kW/m^2 with the vigorous ejection of bubbles from the channels.

Marto and Lepere [18] found that, for the High Flux tube (50 mm length) in R113, once boiling is initiated, the entire test section is active in about 0.015 s. For the Gewa-T and Thermoexcel-E surface, a few sites first become active at some incipient heat flux. Additional sites become active with further increasing heat flux, subsequently activating a complete ring around the cylinder. The rapid initiation of boiling across the High Flux surface was attributed to the interconnecting character of the surface and the high heat capacity of the test section. In the present study, while the spreading of boiling on the smooth tube is gradual, it is stepwise on the enhanced tubes. From Fig. 5b at $q = 10$ kW/m^2, within the first 0.14 s (from $t = 0$ to 0.14 s), the boiling front does not move essentially; then it moves quickly forwards for about 3.1 mm (from $t = 0.14$ to 0.28 s), viz. at a velocity of 22 mm/s; after that it stops again for at least one second (from $t = 0.28$ to 1.27 s). The possible explanation is that, after the rapid initiation of boiling in certain area of channels, the local surface temperature near the boiling front decreases suddenly, therefore it takes a long time to for the temperature to build up in order to push the boiling front forwards.

Tube PB2 shows a similar boiling initiation as PB1. No observation was made for PB4. For PB3, no convection schliere is found (Fig. 6a), instead, big bubbles grow on the pores even at $q = 2$ kW/m^2. This is quite different from PB1&2, since the temperature overshoot for PB3 is similar to that for PB1&2 (Fig. 3 in [1]). This may be due to the fact that the biggest openings on PB3 are much smaller than those on PB1&2 (Fig. 1), thus the outflow of hot liquid from the channels is greatly restricted, therefore, nucleation occurs at certain channel areas in response to the increase of the wall temperature. But a rapid seeding of active nucleation site (by the expansion of individual vapor columns inside channels) is also restricted due to the same reason. Thus, relatively big

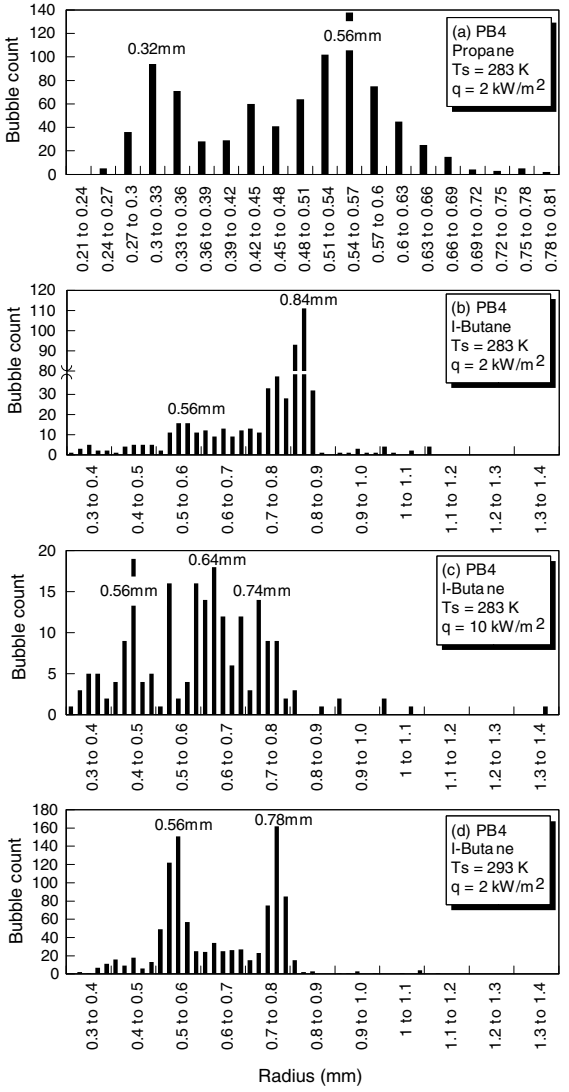

Fig. 3. Bubble radius distributions for boiling of isobutane and propane on PB4.

temperature overshoot still exists at $q = 10\ \mathrm{kW/m^2}$, though bubbles are already seen at $q = 2\ \mathrm{kW/m^2}$.

In fact, a small temperature overshoot exists even at $q > 10\ \mathrm{kW/m^2}$ for mixtures, especially for the smooth tube and PB3 (Fig. 3 in [1]). This is due to the effects of supersaturation and mass diffusion [19] as described in [1]. The trapped vapor nuclei become smaller and consequently many small nuclei are inactive during ascending heat flux, while they become active during descending heat flux. The visualization also shows that, for all enhanced tubes during boiling of mixtures, much more small bubbles are generated for descending heat flux than for ascending heat flux (compare Fig. 6a and b). These small bubbles are partially responsible for

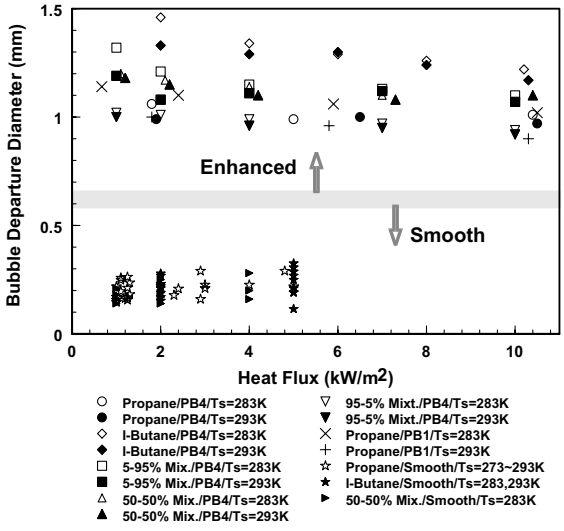

Fig. 4. Bubble departure diameters for smooth tube and enhanced tubes PB1 & PB4.

the difference of wall superheats between ascending and descending heat fluxes.

5. Bubble behavior on enhanced tube PB4

Boiling of mixtures shows a much more distinct heat transfer degradation for the enhanced tubes than for the smooth tube [1]. Here, the effects of mixtures on enhanced boiling will be shown by the bubble behavior on PB4 which has the best heat transfer performance among the tubes investigated.

5.1. Bubble shapes in boiling of different fluids

Fig. 7 shows the comparison of the bubble shapes in boiling of pure components and the 50–50% mixture. Except at the early growth stage, the bubbles show elongated shapes. A noticeable feature is that there is a sharp turn of the curvature of the bubble base for the bubbles growing in the mixtures at the later growth stage (Fig. 7c and d). This phenomenon is probably due to the much higher surface tension of the liquid near the triple-line (the contact line between the bubble interface and the heated wall) than away from it. Note that the surface tension of isobutane is more than 30% higher than that of propane at the temperature of 283 K, and that the surface tension decreases just slightly with increasing temperature (about –0.3%/K). Therefore, it is proposed that there exists a strong concentration gradient at least in the liquid near the triple-line of a growing bubble, which obviously results from the preferential evaporation of the more volatile component. At higher heat

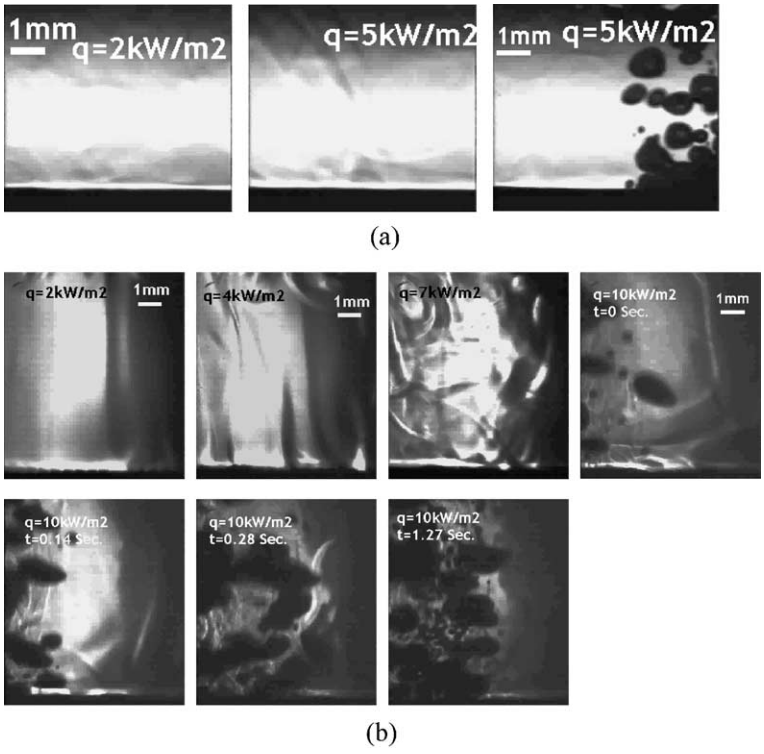

Fig. 5. Natural convection schliere and boiling initiation. (a) Smooth tube, Isobutane, $T_S = 283$ K; (b) PB1, 50–50% mixture, $T_S = 293$ K.

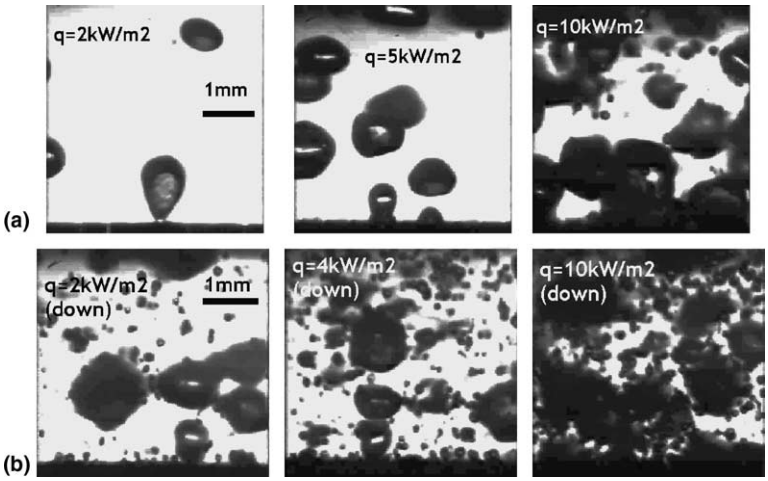

Fig. 6. Different bubble patterns for ascending (a) and descending heat flux (b) (PB3, 50–50% mixture, $T_S = 193$ K).

fluxes, it is reasonable to believe that there is a concentration gradient in the liquid near the heated wall.

In fact, only a very few bubble sequences observed show the shapes given in Fig. 7d. This kind of bubbles is thought to be generated under the following conditions: (1) very low heat flux, which means the liquid convection near the wall is weak; (2) the last one of a series of bubble growth events, thus the liquid near the wall is more likely to be depleted with the more volatile component; (3) slow growth rate, thus the evaporation of the

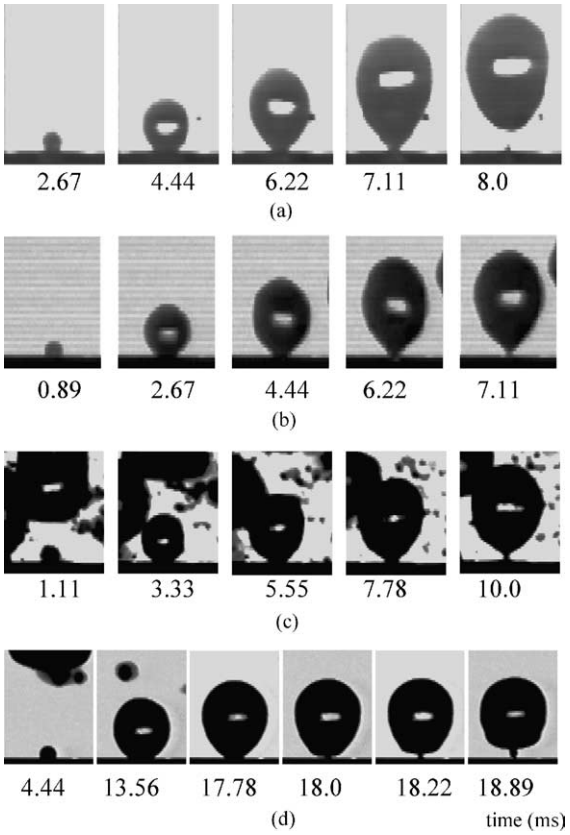

Fig. 7. Bubble shapes in boiling of different liquids on PB4 (for all the bubbles shown, the departure diameter is about 1.3 mm). (a) Propane, $T_s = 283$ K, $q = 4$ kw/m^2. (b) Iso-butane, $T_s = 283$ K, $q = 4$ kw/m^2. (c) 50–50% mixture, $T_s = 283$ K, $q = 4$ kw/m^2 and (d) 50–50% mixture, $T_s = 283$ K, $q = 1$ kw/m^2.

bubble microlayer contributes more to the bubble growth, as a result the liquid near the bubble base is richer in the heavy component.

5.2. Generation of small bubbles

Fig. 8a–e shows the bubble patterns above the top surface of PB4 for five fluids. For isobutane (Fig. 8a) and propane (Fig. 8b), the bubbles are typically around 1 mm in diameter. In contrast, during boiling of mixtures (Fig. 8c–e), besides big bubbles, there are much more small bubbles, especially for the 95–5% and 50–50% mixtures. The number of small bubbles increases with increasing heat flux. The distribution of bubble radius for boiling of the 50–50% mixture is shown in Fig. 9. The number of small bubbles with a diameter less than 0.5 mm is about 18.5 times that of the big bubbles with a diameter bigger than 0.5 mm. The main bubble diameter is about 0.2 mm, which is similar to the size of the bubbles observed on the smooth surface (Fig. 4). In comparison, no bubble with a diameter less than 0.5 mm was detected for the pure liquids (Fig. 3).

Among the fluids used, nucleation of small bubbles on the top surface of PB4 is found (by examining the videos) only for the 50–50% mixture at q>7 kW/m^2. Therefore, there must be other places where these small bubbles are generated. This will be discussed in the next section.

5.3. Bubble patterns on bottom surface

Whether or not a channel is flooded or partially flooded with liquid can be indicated by bubble patterns on the bottom surface, as shown in Fig. 10a–c. For both the pure liquid and the mixtures, big bubbles are dominant at the bottom surface for $q \geqslant 40$ kW/m^2, which indicates that the channels are vapor filled. The jets of small bubbles (<0.5 mm) are also seen, which are probably generated by the collision of the high pressure vapor from the channels with the big bubbles at the bottom surface, as shown schematically in Fig. 11a.

For $q < 40$ kW/m^2, big bubbles (around 1.5 mm) and also small bubbles (<0.7 mm) were observed for propane and the 5–95% mixture (Fig. 10a and b). However, for the 95–5% mixture, the bubbles generally have a diameter less than 0.7 mm with only a few exceptions (Fig. 10c). Jets of small bubbles were found only for the mixtures, which are partially responsible for the large number of small bubbles observed above the top surface.

For the 95–5% mixtures at $q < 40$ kW/m^2, the dominating small bubbles on the bottom surface are not generated by vapor columns as they are on the top surface, but rather by isolated bubbles or small vapor bodies inside the channels. This means that the lower part of the channels is flooded with liquid. Due to the preferential evaporation of propane, the fluid inside the channels has a higher concentration of isobutane, whereby density as well as boiling point of the liquid increase. Thus the liquid columns tend to stay in the lower part of the channels, which tends to prevent the oscillating vapor columns to reach the bottom surface. On the other hand, the temperature of the channel wall occupied by the liquid columns becomes higher, which facilitates the individual nucleation of bubbles. As a result, the liquid has a certain value of vapor quality, which prevents the bubbles near the bottom surface to move upwards. These bubbles then escape through the pores on the bottom surface. When the local pressure is high enough, jets of small bubbles occur. This is shown schematically in Fig. 11b.

For the 5–95% mixture at $q < 40$ kW/m^2, the mechanisms responsible for the generation of jets of small bubbles are the same as described above. However, big bubbles are observed at the bottom surface which indicates that the vapor columns can reach the bottom surface (Fig. 11c).

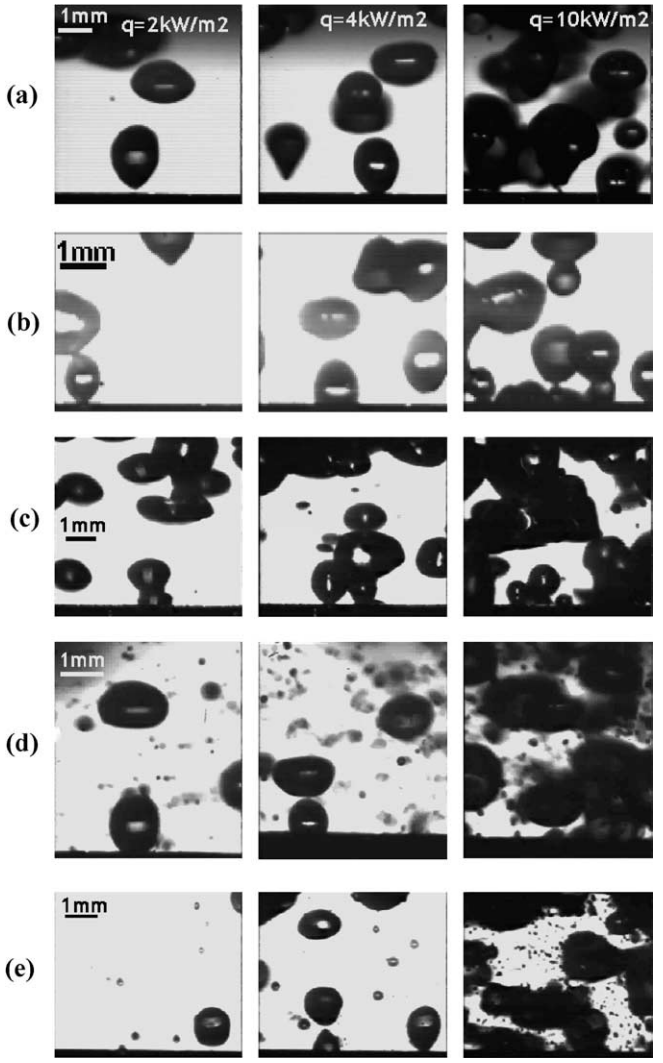

Fig. 8. Bubble patterns above tope surface of PB4 for different fluids. (a) Isobutane, T_s = 283 K. (b) Propane T_s = 283 K, (c) 5–95% mixture, T_s = 283 K. (d) 50–50% mixture, T_s = 283 K and (e) 95–5% mixture, T_s = 283 K.

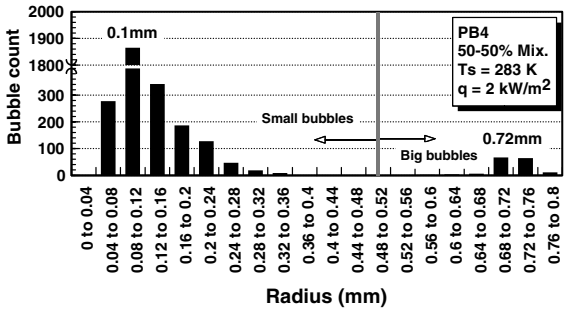

Fig. 9. Bubble radius distributions for boiling of the 50–50% mixture on PB4.

For propane at $q < 40$ kW/m^2, the vapor columns also can reach the bottom surface, however, since there is no jet of small bubbles observed, the liquid columns inside the channels are relatively short and there are fewer nucleation sites (Fig. 11d). In fact, during boiling of methanol on a surface similar to Thermoexcel-E with a transparent cover, Chien and Webb [3] also observed that the channels are partially filled with liquid (10–30%) at $q < 10$ kW/m^2.

It can be concluded from above that more of the channel space is occupied by liquid in boiling of mixtures than in boiling of pure fluids at $q < 40$ kW/m^2. The partial flooding of the channels by the liquid decreases the heat transfer performance of the enhanced tube. This can be seen in Fig. 9c in [1] where, at a heat flux of about 40 kW/m^2 (for T_S = 293 K), the degradation factor of the mixture heat transfer reaches its lowest level.

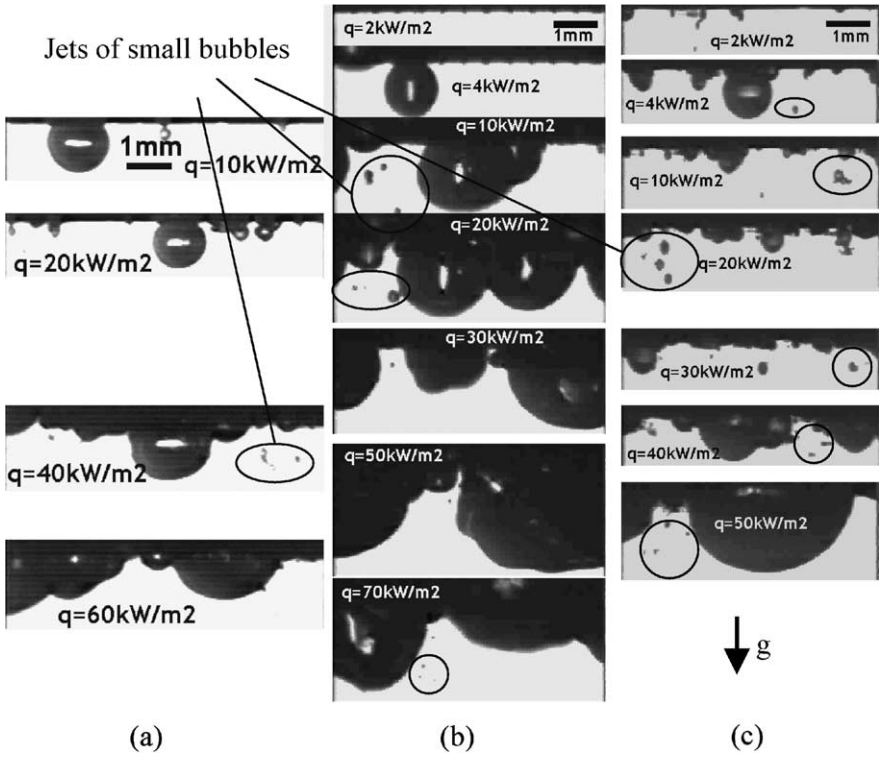

Fig. 10. Bubble growing on the bottom surface of PB4 at T_S = 283 K. (a) Propane. (b) 5–95% mixture and (c) 95–5% mixture.

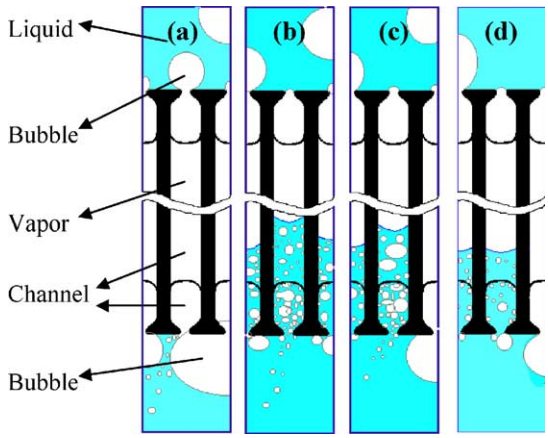

Fig. 11. Channel states indicated by bubble patterns on the bottom surface.

6. Effects of physical properties

Besides the strong effects of mixture, the fluid physical properties also influence the bubble (and channel) behavior and consequently affect the heat transfer performance. Marto and Lepere [18] postulated that the lower improvement factor for enhanced surfaces during boiling of FC-72 compared to that of R113 is due to the lower latent heat of FC-72. In fact, this is true only for relatively high heat fluxes. Since for a given amount of heat for vaporization, the higher the product of latent heat and vapor density, the lower the volume of vapor generated. Thus the channels will easier be flooded with liquid at relatively low heat fluxes, as it has already been shown that the channels are easier to be flooded for the 95–5% mixture than for the 5–95% mixture at $q < 40$ kW/m^2 (refer Fig. 10b and c). Note that the product of latent heat and vapor density for the 95–5% mixture at T_S = 283 K is about 2.2 times higher than that for the 5–95% mixture, it is 2.4 times higher for propane than for isobutane. However, at high heat fluxes, the channels are easier to be dried-out for the fluid with lower product of latent heat and vapor density, which will also impair the heat transfer performance. This can be seen from Figs. 5–8 in [1] that, for a given enhanced tube, propane performs better at high heat fluxes than isobutane, and the latter generally performs better at low heat fluxes.

Another important parameter is surface tension. The higher surface tension of isobutane than propane leads to the fact that the isobutane bubbles are bigger than the propane bubbles (Fig. 4) and that small bubbles (around 0.2 mm) are not easy to generate on the

enhanced tubes (without sufficiently high wall superheat). This is also true for the comparison between the 5–95% and 95–5% mixtures.

7. Bubble behavior on different enhanced surfaces

In fact, for the reentrant surfaces, the effects of mixture and fluid properties are strongly related to the surface geometries, this will be shown in the following for the tubes PB1, PB2 and PB3.

7.1. Tube PB1

PB1 is more similar to a finned tube and has a much bigger slit than the other tubes (Table 2 in [1]). Fig. 12a–c show the bubble patterns on the bottom surface for boiling of isobutane, the 5–95% and 95–5% mixtures, respectively. For the two mixtures, many fin gaps are filled with liquid for $q < 50\ \mathrm{kW/m^2}$, while this is not found for isobutane at least (only available) for $q \geqslant 15\ \mathrm{kW/m^2}$. This indicates that more channel area is flooded during boiling of the mixtures than during boiling of isobutane.

For the 95–5% mixture (Fig. 12c), small bubbles growing on the fin tips are dominant for $q < 50\ \mathrm{kW/m^2}$, while big bubbles begin to be seen at $q = 10\ \mathrm{kW/m^2}$, this does not occur for PB4 until at $q = 40\ \mathrm{kW/m^2}$ (Fig. 10c). It would be strange if this means that more channels are completely vapor filled for PB1 than for PB4, since the big fin gaps of PB1 are not favorable for retaining vapor columns inside the channels (it is also not supported by

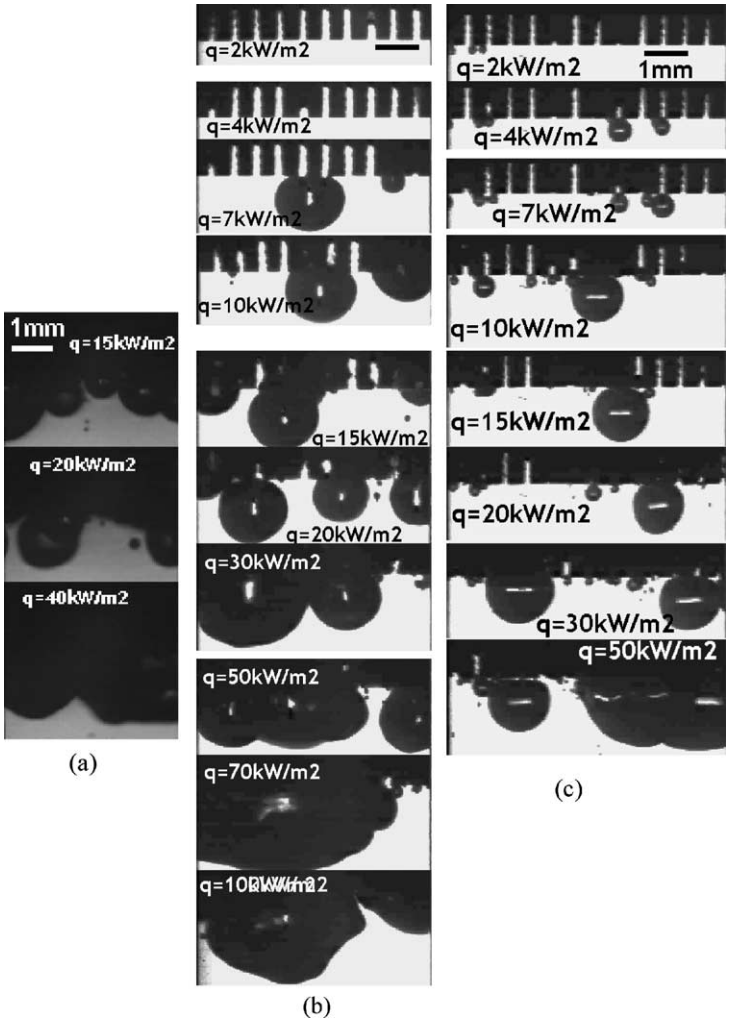

Fig. 12. Bubble patterns on the bottom surface of PB1 for boiling of isobutane (a), 5–95% mixture (b) and 95–5% mixture (c) ($T_S = 283$ K).

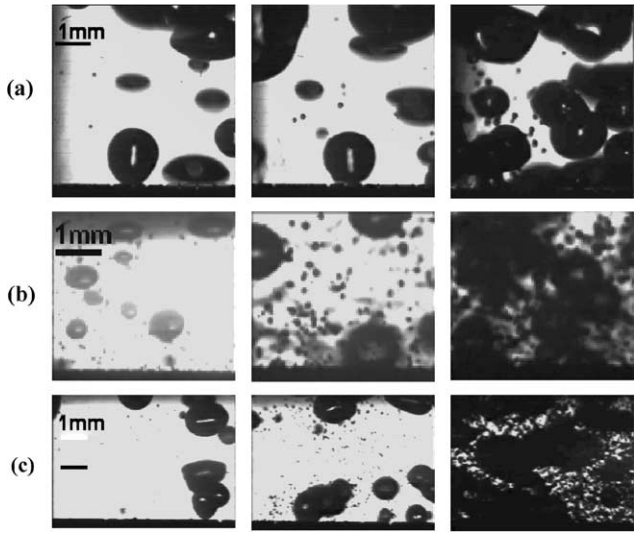

Fig. 13. Bubble patterns above tope surface of PB1 for the mixtures (T_S = 283 K). (a) 5–95% mixture. (b) 50–50% mixture and (c) 95–5% mixture.

the results of heat transfer performance [1]). In fact, for PB1, jets of small bubbles are rarely seen due to the big fin gaps. This also indicates that, compared to PB4, the channel pressure is more difficult to be built up and the oscillation of liquid and vapor inside the channels induced by the pumping action of bubbles on the outer surface is weaker. Therefore, for PB1 at relatively low heat fluxes, a big bubble can grow and detach on the bottom surface without being moved upwards alone the channel. Thus, the big bubbles on the bottom surface do not necessarily indicate that the corresponding channels are vapor filled, they can be generated from liquid-filled channels as those generated from the bottom surface of the smooth surface. This is also true for the 5–95% mixture (Fig. 12b).

In boiling of mixtures, more small bubbles are observed for PB1 (Fig. 13) than for PB4 (Fig. 8). Since many of the channels are partially liquid filled, the contribution of superheated liquid inside the channels taken away by the pumping action of small bubbles may be great, as it is in the case of boiling on the smooth surface. This may be the reason that the degradation factor for the 95–5% mixture is higher than for the 5–95% mixture for $q < 50$ kW/m^2, since the former has a much larger number of small bubbles than the latter (Figs. 12 and 13).

7.2. Tube PB2

For PB2, the regularly distributed very big pores facilitate the supply of liquid into the channels and also the flowing out from the channels, thus for the mixtures, the clogging of the heavier component inside the channels can be avoided; however, for the pure fluids, the channels are easier flooded at least for the low heat fluxes which leads to a reduced heat transfer performance (PB2 has the best performance for the 50–50% mixture, but the worst for the pure components, Fig. 10 in [1]). Fig. 14 shows the bubble patterns on the bottom surface of PB2 during boiling of propane. The generation of solely small bubbles at $q < 30$ kW/m^2 indicates that the vapor column cannot reach the bottom and that the channels are partially flooded (compare to Fig. 10a).

7.3. Tube PB3

In contrast to PB1&2, PB3 has very small openings (slits), thus the supply of liquid into the channel is greatly limited. For the 50–50% mixture, the escape of the light component (low surface tension) happens through the generation of small and medium sized bubbles (Fig. 15a), leaving the heavier component clogged

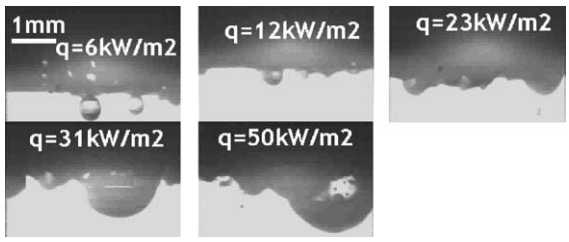

Fig. 14. Bubble patterns on the bottom surface of PB2 for boiling of propane (T_S = 293 K).

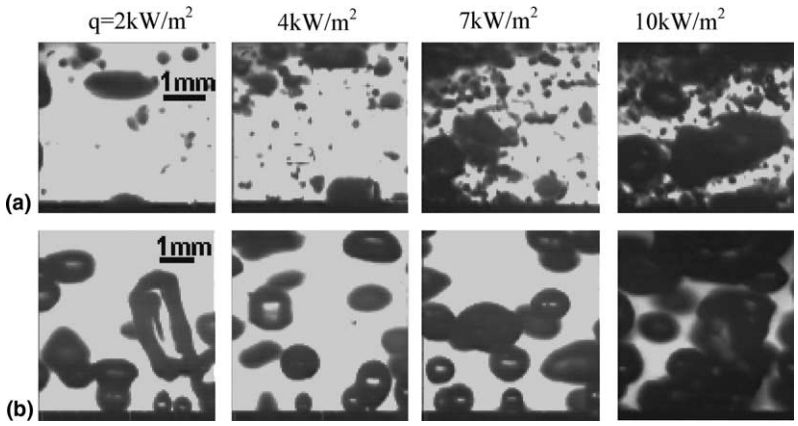

Fig. 15. Bubble patterns on the top surface of PB3: (a) 50–50% mixture; (b) Isobutane (T_S = 283 K).

inside the channel. As a result, the heat transfer performance of the 50–50% mixture is the worst one (Fig. 10 in [1]). However, for isobutane, since the product of latent heat and vapor density is low and, the surface tension is relatively high, the channel vapor pressure is easier to be built up. As a result, thin-film evaporation can happen even at low heat fluxes, and the wall superheat can be kept at a low level, especially at low heat fluxes. This is supported by the typical picture shown in Fig. 15b, where many big bubbles are seen even at a heat flux of 2 kW/m^2. However, with increasing heat fluxes, the inability of evacuating the vapor from the channels limits the further improvement of the heat transfer performance. Thus the heat transfer coefficient shows the surprising independence on the heat flux (Fig. 8 in [1]).

The high performance of **PB4** apparently benefits from its surface geometry, viz., not very big pores (compared to those of PB2) connected by small slits, instead of continuous circumferential slits as for PB1 and PB3.

7.4. Generation of small bubbles

As described in Section 4, the generation of small bubbles (<0.5 mm) generally indicates that there are liquid columns inside the channels and that nucleation happens on the channel wall and/or on the outer surface, therefore this is not an optimal operation condition for heat transfer. For the four enhanced tubes used, a summary is given as follows based on observations of video pictures including those already shown above:

(1) No small bubbles are observed during boiling of isobutane for all tubes, which is mainly due to the high surface tension of isobutane.
(2) During boiling of propane at $q > 20$ kW/m^2, small bubbles are observed which, however, are not generated by nucleation on the surfaces but by the interactions of big bubbles.
(3) Small bubbles are observed for all tubes during boiling of mixtures, however, very few are found for boiling of the 5–95% mixture on PB4.
(4) For the 50–50% mixture, nucleation on the top surface happens for all tubes.
(5) For PB4, nucleation on the top surface happens only for the 50–50% mixture; while for the other enhanced tubes, nucleation on the top surface happens for all mixtures tested.
(6) These results support the fact that PB4 is generally the tube with the best performance and that the 50–50% mixture is the fluid with the worst performance. The large number of small bubbles generated during boiling of mixtures may be also related to the Marangoni effect. Since the propane/isobutane mixtures are positive mixtures in which the surface tension is smaller for the light component than for the heavy component. Thus the coalescence of bubbles is restrained by the Marangoni convection [20].

8. Conclusions

(1) Mixture effects strongly influence nucleation and evaporation processes which are significantly different from those during boiling of pure fluids. For the mixtures, natural convection schliere is observed even for the enhanced surfaces; the sharp turn of the curvature of the bubble base proves indirectly the existence of mass transfer effects; the large number of small bubbles generated either on the outer non-pore surface area or from inside the sub-surface channels of the enhanced tubes is a clear indication that the surface temperature is higher and more channel area is flooded than it would be during boiling of pure fluids. The generation of small bubbles may also be partially attributed to the Marangoni convection.

(2) The fluid physical properties also influence the bubble behavior and consequently affect the heat transfer performance. The product of latent heat and vapor density prescribes the vapor volume which can be generated by a given heat input. This directly affects the channel behavior. The higher this product, the easier the channels will be flooded and the less likely dry-out occurs. Surface tension shows the influences on the bubble size and nucleation and, to a lesser extent, on channel behavior.

(3) The effects of reentrant enhanced surface geometries are complicated and closely related to mixture effects, fluid properties and working conditions. In general, for a surface with big openings (e.g. PB1 and PB2), the channels are easier to be flooded at low heat fluxes. For a surface with small openings (e.g. PB3), the channels are easier clogged with the vapor phase at high heat fluxes, which will also reduce the heat transfer performance. The reentrant surface having not very big pores which are connected by small slits (e.g. PB4) is superior, in terms of boiling heat transfer performance, over those having practically circumferential slits (e.g. PB1 and PB3). For mixtures, relatively big surface openings (e.g. PB2) facilitate the driving out of the heavy component fluid from the channels and thus give a better heat transfer performance.

Acknowledgments

This work has been partially funded by the Commission of the European Community. The financial support from Friedrich-Ebert-Stiftung for the doctoral study of one of the authors, Yuming Chen, is greatly appreciated.

References

[1] Y. Chen, M. Groll, R. Mertz, R. Kulenovic, Pool boiling heat transfer of propane, isobutane and their mixtures on enhanced tubes with reentrant channels, Int. J. Heat Mass Transfer, in press.

[2] W. Nakayama, T. Daikoku, T. Nakajima, Effects of pore diameters and system pressure on saturated pool nucleate boiling heat transfer from porous surfaces, J. Heat Transfer 104 (1982) 286–291.

[3] L.-H. Chien, R.L. Webb, Visualization of pool boiling on enhanced surfaces, Exper. Thermal Fluid Sci. 16 (1998) 332–341.

[4] Y. Chen, M. Groll, R. Mertz, R. Kulenovic, Comparison of pool boiling bubble dynamics on smooth and enhanced tubes, Int. J. Heat & Technol. 20 (2002) 3–14.

[5] W. Nakayama, T. Daikoku, H. Kuwahara, T. Nakajima, Dynamic model of enhanced boiling heat transfer on porous surfaces, Part I: Experimental investigation, J. of Heat Transfer 102 (1980) 445–450.

[6] R.R. Trewin, M.K. Jensen and A.E. Bergles, Pool boiling from enhanced surface in pure and binary mixtures of R-113 and R-11, in: Proc.10th Int. Heat Transfer Conf., UK, 1994, pp. 165–170.

[7] J. Arshad, J.R. Thome, Enhanced boiling surfaces: Heat transfer mechanism and mixture boiling, in: Proc. ASME-JSME Therm. Eng. Joint Conf., vol. 1, 1983, pp. 191–197.

[8] Z.H. Ayub, A.E. Bergles, Pool boiling from GEWA surfaces in water and R-113, Wärme- und Stoffübertragung 21 (1987) 209–219.

[9] S.B. Memory, D.C. Sugiyama, P.J. Marto, Nucleate pool boiling of R-114 and R-114—oil mixtures from smooth and enhanced surfaces — I. Single tubes, Int. J. Heat Mass Transfer 38 (1995) 1347–1361.

[10] J.R. Thome, Enhanced boiling of mixtures, Chem. Engng. Sci. 42 (8) (1987) 1909–1917.

[11] J.R. Thome, Enhanced boiling heat transfer, Hemisphere (1990).

[12] P.S. O'Neill, C.F. Gottzman, J.W. Terbot, Novel heat exchanger increases cascade cycle efficiency for natural gas liquefaction, Adv. Cryogenic Engng. 17 (1972) 420–437.

[13] G. Barthau, Active nucleation site density and pool boiling heat transfer—an experimental study, Int. J. Heat Mass Transfer 35 (1992) 271–278.

[14] H. Auracher, W. Marquardt, New experimental results in boiling heat transfer, in: Celata, G.P. et al. (Eds.), Exper. Heat Transfer, Fluid Mech. Thermodynam., 2001, pp. 119–128.

[15] L.-H. Chien, R.L. Webb, A parametric study of nucleate boiling on structured surfaces, Part I: Effect of tunnel dimensions, J. Heat Transfer 120 (1998) 1042–1048.

[16] L.-H. Chien, R.L. Webb, A parametric study of nucleate boiling on structured surfaces, Part II: Effect of pore diameter and pore pitch, J. Heat Transfer 120 (1998) 1049–1054.

[17] T. Ma, X. Liu, J. Wu, H. Li, Effects of geometrical shapes and parameters of reentrant grooves on nucleate pool boiling heat transfer from porous surfaces, in: Proc. 8th Int. Heat Transfer Conf., 4 (1986) 2013–2018.

[18] P.J. Marto, Lt. V.J. Lepere, Pool boiling heat transfer from enhanced surfaces to dielectric fluids, J. Heat Transfer 104 (1982) 292–299.

[19] S. Shakir and J.R. Thome, Boiling nucleation of mixtures on smooth and enhanced boiling surfaces, in: Proc. 8th Int. Heat Transfer Conf., 4 (1986) 2081–2086.

[20] Y. Fujita, Q. Bai, Critical heat flux of binary mixtures in pool boiling and its correlation in terms of Marangoni number, Int. J. Refrig. 20 (8) (1997) 616–622.